Structural Engineering and Mechanics, Vol. 5, No. 2 (1997) 193-207
DOI: http://dx.doi.org/10.12989/sem.1997.5.2.193

Inelastic general instability of ring-stiffened circular cylinders and cones under uniform external pressure

C.T.F. Ross†

Department of Mechanical and Manufacturing Engineering, University of Portsmouth, Portsmouth, England

Abstract. Experimental tests are described on three ring stiffened machined circular cylinders and three ring stiffened machined circular cones, which were tested to destruction under uniform external pressure. All six vessels failed by inelastic general instability. The experiments showed that the vessels initially deformed plastically at mid-bay in the circumferential direction, and this caused the circumferential tangent modulus to become much less than the elastic Young's modulus, causing the vessels to fail through plastic general instability at pressures much less than that predicted by elastic theory. Based on a thinness ratio, two semi-empirical design charts are provided, which are intended to be used for design purposes in conjunction with the finite element method and a plastic reduction factor.

Key words: cylinders; cones; instability; external pressure

1. Introduction

The study of the general instability of ring-stiffened circular cylinders and cones 1 to 9 under uniform external pressure is of much importance in the design of submarine structures, off-shore drilling rigs, torpedoes, water-borne ballistic missiles, tunnels and immersed tubes.

When such structures are subjected to uniform external pressure, they can fail by shell instability, at a pressure which may be a small fraction of that to cause axisymmetric yield, as shown in Fig. 1.

One method of improving the structural efficiency of these vessels, is to stiffen them with ring stiffeners, spaced at suitable distances apart.

If, however, the ring stiffeners are not strong enough, the entire ring-shell combination can fail bodily, as shown in Figs. 2 and 3. This mode of failure is known as general instability.

Much work has been done on the general instability of ring-stiffened circular cylinders 1 to 8, but not as much on the general instability of ring-stiffened circular cones 8, 9. The main findings of these studies is that good agreement was found between experiment and theory for long slender vessels, but agreement between experiment and theory was poor for less slender vessels. The reasons for this is that in some cases, the initial out-of-circularity of a vessel, can cause a catastrophic decrease in the value of the buckling pressure, based on elastic instability theory of an initially perfect vessel. For thicker vessels, with very small initial out-of-circularity, the vessels can initially deform plastically, in an axisymmetric manner, causing the circumferential

† BSc, PhD, DSc

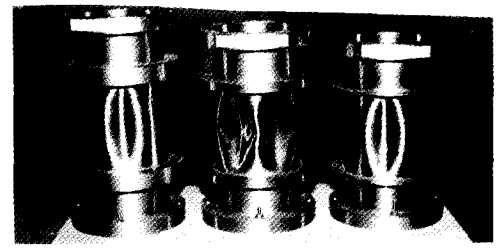

Fig. 1 Shell instability.

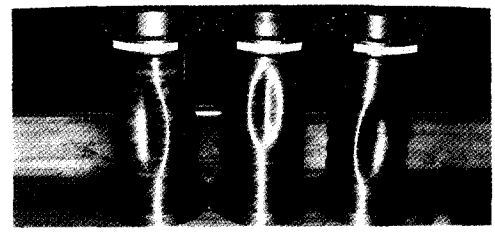

Fig. 2 General instability of ring-stiffened circular cylinders.

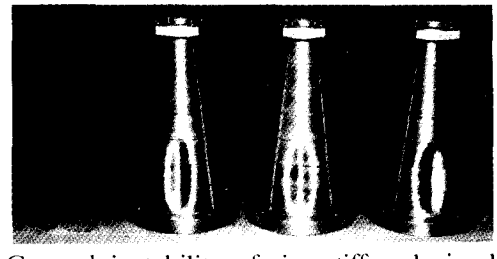

Fig. 3 General instability of ring-stiffened circular cones.

tangent modulus to decrease, so that failure takes place due to plastic general instability, at a pressure much less than that to theoretically cause elastic general instability.

One method of analysing the inelastic instability of these vessels is by the finite element method, as carried out by Bosman, *et. al.* (1993).

However, in the case of the successful analysis of Bosman, *et al.*, which allowed for geometrical and material non-linearity, their models had very large values of initial out-of-circularity. The initial out-of-circularity of their models varied from 0.4438 mm to 0.6755 mm, which was considerably larger than the initial out-of-circularity of the present series of models, which did not exceed 0.013 mm; that is, the worst initial out-of-circularity of the present series of models was only about 1/50th of that of the models of Bosman, *et. al.* The models of Bosman, *et. al.* had diameters which were slightly larger than twice the diameters of the present series.

Additionally, the shape of the initial out-of-circularity of the models of Bosman, *et. al.*, in the circumferential directions, was made to be of a sinusoidal shape, to maximise the detrimental effects of initial out-of-circularity; for the present series of vessels, the shape of the circumferential initial out-of-circularity was quite random.

It is believed that for the present series of models, where the worst initial out-of-circularity was of random shape and of a magnitude not exceeding 0.013 mm, the vessels initially became

plastic in the circumferential direction and this caused the circumferential tangent modulus to decrease, resulting in a plastic general instability mode of failure.

In this paper, a semi-empirical method is suggested, which is based on the thinness ratio "λ" of Windenburg and Trilling (1934). For both the ring-stiffened circular cylinders and the ring-stiffened circular cones, a thinness ratio λ' (Ross 1990) is used, where λ' is for an unstiffened circular cylinder of "equivalent strength" to the ring-stiffened cylinder or cone. Naturally of course, this equivalent cylinder will have a slightly larger wall thickness than the original ring-stiffened cylinder or cone, to allow for the strength of the stiffening rings. The method of calculating λ' for both vessels is given below.

λ' for a ring-stiffened circular cylinder
This was first presented by Ross in (1990)

$$\lambda=[(L_b/D_f)^2/(t'/D_f)^3]^{0.25}\sqrt{[\sigma_{yp}/E]}$$

L_b =length of ring-stiffened cylinder between adjacent bulkheads.
D_f =diameter of the centroid of a typical ring-shell combination
t' =equivalent shell thickness
σ_{yp} =yield stress
E =Young's modulus

A typical ring-shell combination for model P_1 shown in Figs. 4 and 5.

h =1.56 L_b=204.64

Internal diameters=101.6
The material properties of the vessel were found to be as shown below:

E =Young's modulus=200 GPa

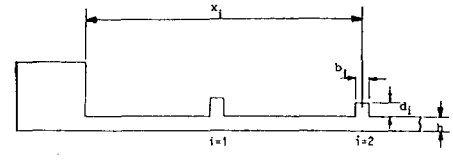

i	Model P1		
	x_i	d_i	b_i
1	1.273	2.04	1.57
2	30.55	1.53	1.56
3	54.59	1.53	1.61
4	78.43	1.53	1.57
5	102.35	1.53	1.56
6	126.25	1.53	1.54
7	150.16	1.53	1.57
8	174.08	1.53	1.57
9	191.91	2.04	1.57

Fig. 4 Model P_1 (mm).

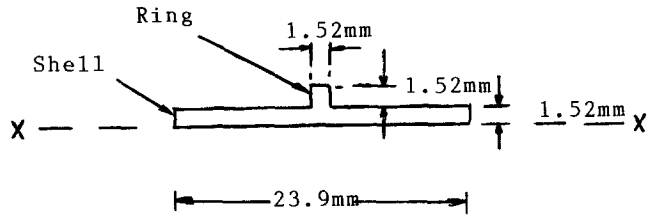

Fig. 5 Typical ring-shell combination.

σ_{yp} =yield stress=162 MPa
Nominal peak stress=336 MPa

To demonstrate how to calculate λ', D_f and t', a detailed calculation for Model P1 (Ross 1990, Ross, Aylward and Boltwood 1971) will now be made.

A =area of section
$=23.88\times1.52+1.52\times1.52$
A $=38.61$ mm^2
$\bar{y}$ =distance of centroid of a typical ring-shell combination from the axis $x-x$
$=0.853$ mm
I_{xx} =second moment of area of a typical ring-shell combination about the axis $x-x$
$=40.77$ mm^4
I =second moment of areas of a typical ring-shell combination about its own centroid and parallel to $x-x$
$=I_{xx}-\bar{y}^2\times A$
$\therefore I$ $=12.57$ mm^4

and

D_f $=(50.8+\bar{y})\times2=103.3$ mm
If t'=the thickness of an "equivalent" unstiffened section.
t' $=[12.57\times12/23.88]^{0.333}$
$\therefore t'$ $=1.85$ mm

Now from reference Ross (1990)

E $=200$ GPa
σ_{yp} $=162$ MPa
L_b $=204.7$ mm
Hence, $\lambda'=0.816$

1.1. λ' for a ring-stiffened circular cone

The formula for λ' for ring-stiffened circular cylinders also applies to ring-stiffened circular cones, but some of the definitions are somewhat different, as shown by Figs. 6 and 7.

It should be noted from Figs. 6 and 7, that the slant lengths of the cones are used to calculate λ' for the ring-stiffened cone.

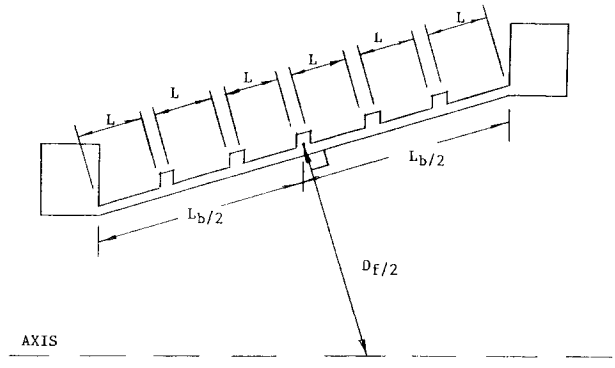

Fig. 6 Ring-stiffened cone.

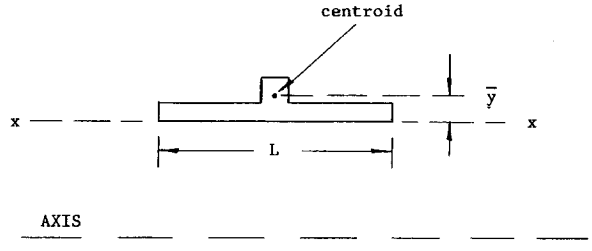

Fig. 7 "Equivalent" ring-shell combination for a cone.

2. Apparatus

All the models were machined from a solid billet of EN1A steel. First of all, the inside surfaces of each model were bored out, and then, each model was placed, in turn, on a mandrel. The outer surface of each model was then machined very carefully. All the models were designed to fail by general instability.

2.1. Cylinders

Details of the geometrical properties of the three ring-stiffened cylinders, namely P4, P5 and P6 are shown in Fig. 8 and a photograph of the models is shown in Fig. 9.

The initial out-of circularity of the models was very small and of random shapes around the circumferences of the vessels. The initial out-of-circularity for model P4 was 0.013 mm, for model P5 it was 0.0069 mm and for model P6 it was 0.0079 mm. That is, worst initial out-of circularity was 0.013 mm.

The initial out-of-circularity was obtained by first obtaining a mean circle at the external surface at mid-bay, through a least squares' fit with the aid of a Mitutoya co-ordinate measuring machine and a tough-trigger probe. The initial out-of-circularity was then defined as half the difference between the maximum inward and outward radial deviations of each vessel on the external surface at mid-bay from this mean circle.

The material properties of these vessels were as follows:-

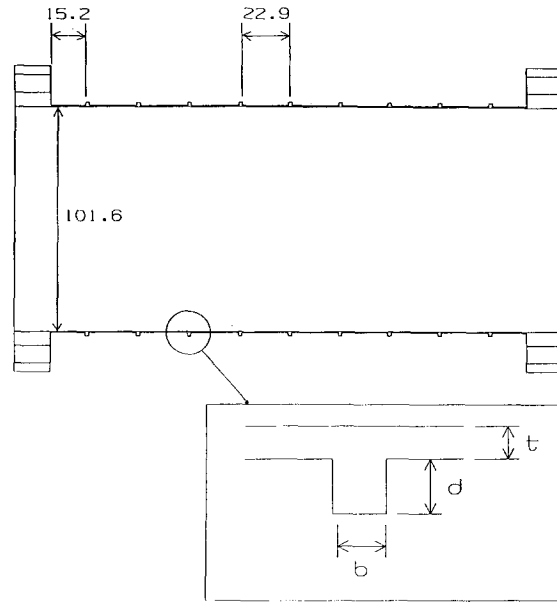

Cylinder	b	d	t	N
P4	1.6	1.5	1.125	9
P5	1.6	2.0	1.125	9
P6	1.6	2.5	1.125	9

Fig. 8 Details of cylinders P4, P5 and P6.
N=number of ring stiffeners.
All dimensions are in mm.

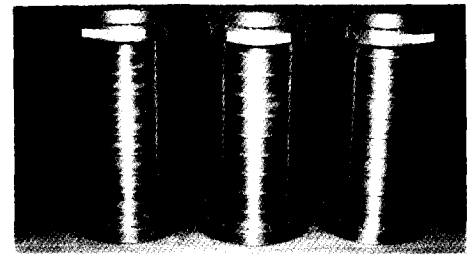

Fig. 9 Models P4, P5 and P6.

σ_{yp} =yield stress=210 MPa
E =Young's modulus=200 GPa
ν =Poisson's ratio=0.3 (assumed)

2.2. Cones

Details of six machined stiffened thin-walled circular cones are shown in Fig. 10, and Table 1, and a photograph of the models 4, 5 & 6 is shown in Fig. 11. The experimental details

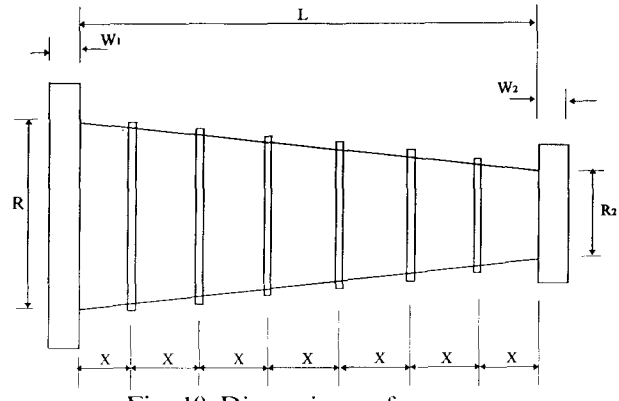

Fig. 10 Dimensions of cones.

Table 1 Dimensions of cones (mm)

Dimensions	Cones 4, 5 and 6
L	211.0
W_1	10.00
W_2	10.00
R_1	38.10
R_2	101.6
X	30.14

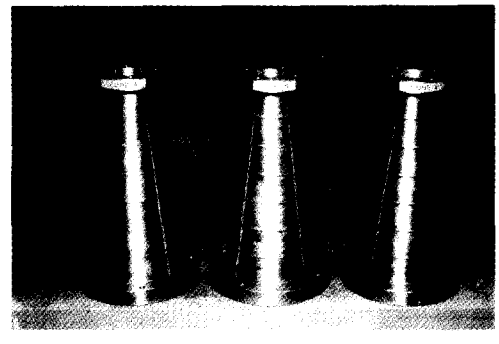

Fig. 11 Cones 4, 5 and 6.

of cones 1, 2 & 3 have been reported elsewhere (Ross 1990).

The initial out-of-circularity for the cones was very small and found to be of a random shape.

The initial out-of-circularity was measured mid-way between stiffeners 1 and 2, on the external surfaces of the vessels. The initial out-of-circularity for Cones 4, 5 and 6 were found to be 0.0076 mm, 0.0054 mm and 0.0064 mm.

The definition of the initial out of circularity was the same as that adopted for the circular cylinders.

Experimental details of Cones 1 to 3 were reported elsewhere (Ross 1990, 1988) and in this report, the experimental details of Cones 4 to 6 are reported.

The material properties of the three vessels were found to be as follows:-

E =190 GPa ,
σ_{yp} =238 MPa , Measured
ν =0.3 (assumed)

2.3. The test tank

The test tank is shown schematically in Fig. 12.

3. Experimental procedure

3.1. Cylinders P4, P5 and P6

Ten linear strain gauges were fitted in the circumferential direction, on the inside surface of each vessel, at its mid-length, under the central ring stiffener. The purpose of these strain gauges was partly to detect the lobar pattern at buckling and partly to observe the inelastic behaviour of each vessel when failing under uniform external pressure.

The first strain gauge recordings were taken at intervals of 6.897 bar, up to 34.48 bar, the pressure was then decreased to zero to detect any drift of the strain gauges; virtually no drift was found.

For the final test to destruction of each vessel, the pressure was increased in increments of 6.897 bar, without reverting to zero. When the expected buckling pressures were approached, the pressures were increased in progressively smaller steps, until failure occurred. All three vessels failed by general instability, as shown by Fig. 2.

A typical plot of the variation of strain gauge readings with external pressure are shown in Fig. 13, and plots of the variation of strain gauge readings around the circumference of each

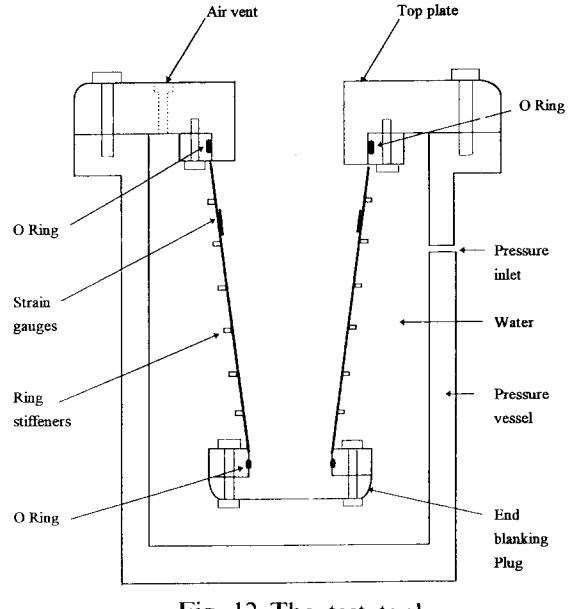

Fig. 12 The test tank.

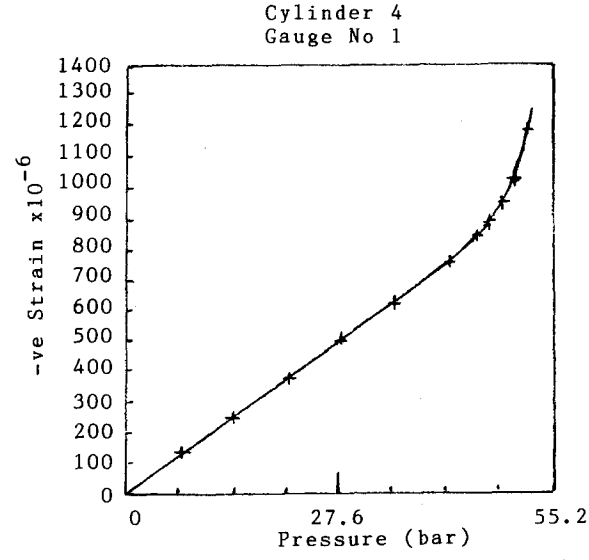

Fig. 13 Variation of strain with pressure for cylinder P4.

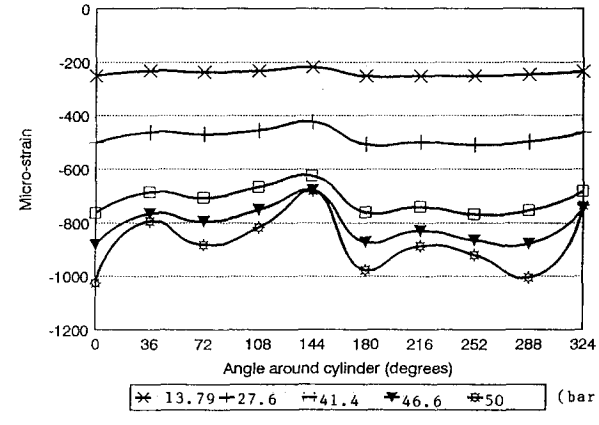

Fig. 14 Circumferential strain readings for cylinder P4.

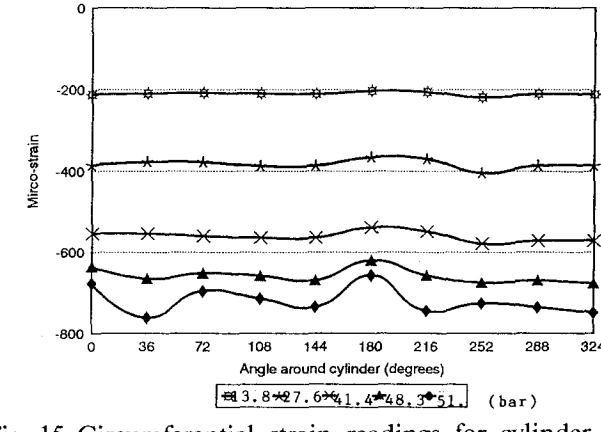

Fig. 15 Circumferential strain readings for cylinder P5.

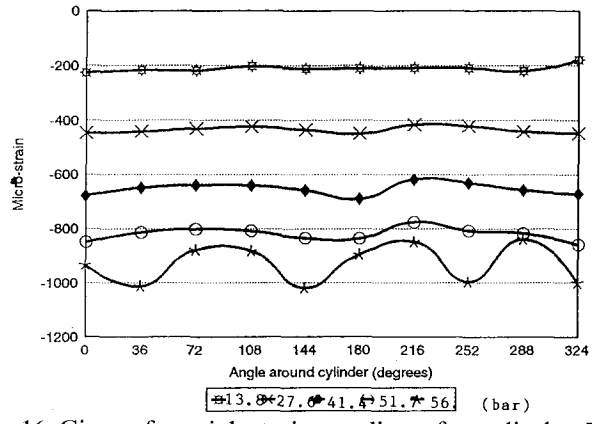

Fig. 16 Circumferential strain readings for cylinder P6.

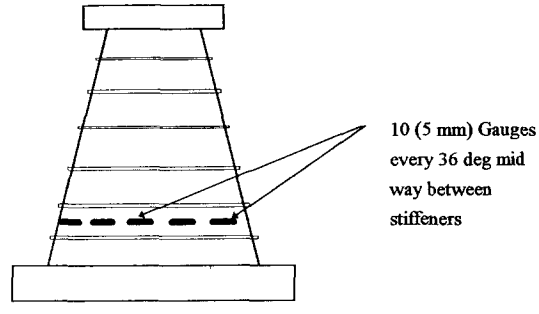

Fig. 17 Positions of strain gauges on Cone 4.

vessel are shown in Figs. 14 to 16.

3.2. Cones 4, 5 and 6

The larger end of each cone was attached to the tank top and the smaller end of each vessel was sealed off by a closure plate, with the aid of four bolts, as shown in Fig. 12.

It was expected that the area of collapse of Cone 3 would be centred between rings 2 and 3, and because of this, eight evenly spaced linear strain gauges were attached to the inner circumference of this vessel, in a circumferential direction, in the position shown by Fig. 17.

The area of collapse, however, for this vessel was centred between rings 1 and 2, and because of this, ten linear strain gauges were attached to the inner circumferences of Cones 5 and 6, in this position; it was possible to attach 10 strain gauges to Cones 5 and 6, because the diameter of these cones was larger at the point between rings 1 and 2, than the diameter at the point between rings 2 and 3 for Cone 4.

The experimental procedure for Cones 4, 5 and 6 was similar to that for Cylinders P4, P5 and P6. Cone 4 failed by general instability at a pressure of 51.75 bar. Although the ring stiffeners for Cone 5 were deeper than that for Cone 4, Cone 5 also failed by general instability at a pressure of 51.75 bar. Cone 6 failed by general instability at a pressure of 54.1 bar.

Plots of the variation of hoop strain around the circumference of each vessel, near their collapse

pressures, are shown in Figs. 18 to 20. These figures also show the maximum inward position of the buckle that occurred for each vessel.

The experimental buckling pressures for the six vessels are shown in Table 2. It was not possible to determine the number of lobes "n" that the cones buckled into.

3.3. Design curves

The design curves will be obtained by plotting λ' against P_{cr}/P_{exp}, for each series of vessels, where

P_{cr}=elastic instability buckling pressure for a perfect vessel
P_{exp}=experimental buckling pressure
P_{cr}/P_{exp}=plastic knockdown factor; to be used for design purposes.

The theoretical values for buckling pressure, namely P_{cr} were obtained by the finite element method, using the conical shell element and ring stiffener element of Ross (1976), (1990).

Table 3 gives values for the elastic knockdown factor and λ' for cylinders P4, P5 and P6, and Table 4 gives values for similar constants for Cones 4, 5 and 6, together with Cones 1, 2 and 3.

A plot of λ' against P_{cr}/P_{exp} is made in Fig. 21 for Cylinders P4, P5 and P6, together with

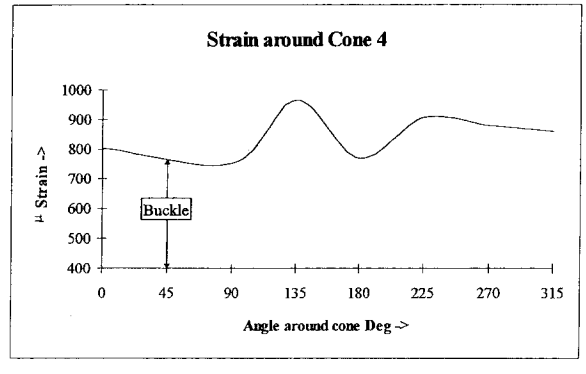

Fig. 18 Variation of circumferential strain for Cone 4.

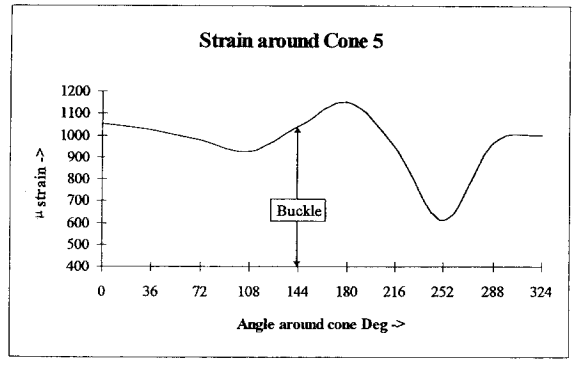

Fig. 19 Variation of circumferential strain for Cone 5.

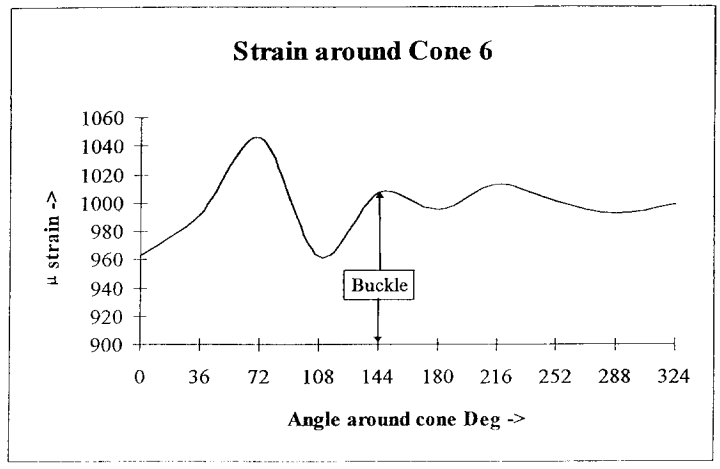

Fig. 20 Variation of circumferential strain for Cone 6.

Table 2 Experimental buckling pressure (P_{exp}) for cylinders and cones

Vessel	P_{exp} (bar)
Cylinder P4	51.72 (4)
Cylinder P5	55.17 (3)
Cylinder P6	58.28 (3)
Cone 4	51.75
Cone 5	51.75
Cone 6	54.11

(The figures in parentheses represent the number of circumferential waves the vessels buckle into).

the results obtained from the machined models of Reynolds and Blumenberg (1959) and Ross (1990). In Fig. 21, a proposed design curve is shown for vessels with slightly larger out-of-circularity/equivalent thickness values, the design curve will lie somewhat higher than the proposed design curve. That is the design curve of Fig. 25 is unconservative, except for slender vessels which are less affected by initial out-of-circularity.

In Fig. 21, it can be seen that was some scatter for the models of Reynolds and Blumenberg (1959), but this might have been because of the experimental boundary conditions for their Case IV, where the vessels were heavily clamped at their ends. Ignoring these results, it appears that elastic general instability of perfect vessels may occur for a value of λ' above 1.8, and these vessels are less affected by initial out-of-circularity.

A plot of λ' against (P_{cr}/P_{exp}) is made for Cones 1 to 6 in Fig. 22. This curve can be regarded as being suitable for perfect vessels. For vessels with larger values of out-of-circularity/equivalent thickness, the design curve will be somewhat higher than the dashed curved of Fig. 22, except perhaps for vessels whose λ' is above 1.8.

Although there was some scatter in Fig. 22, it like Fig. 21, could be useful for design purposes.

The design process would be to calculate P_{cr} by the finite element method and then to divide P_{cr} by the plastic knockdown factor, namely P_{cr}/P_{exp}, to obtain the required inelastic buckling pressure. For vessels with larger initial out-of-circularity/equivalent thickness ratios, the design curve should be higher than that obtained for machined models in Figs. 21 and 22.

Table 3 Buckling pressures (bar) and λ' for cylinders

Cylinder	P_{cr}	P_{exp}	P_{cr}/P_{exp}	λ'
P4	72.76 (3)	51.72 (4)	1.41	1.36
P5	91.66 (3)	55.17 (3)	1.66	1.23
P6	119.66 (3)	58.28 (3)	2.05	1.12

Table 4 Buckling pressures (bar) and $\lambda\pm$ for cones

Cone	P_{cr}	P_{exp}	P_{cr}/P_{exp}	λ'
1	35.5 (4)	29.8 (4)	1.19	1.717
2	54.8 (4)	39.3 (4)	1.39	1.417
3	66.5 (3)	41.0 (3, 4)	1.62	1.271
4	87.99 (3)	51.8	1.70	1.341
5	103.5 (3)	51.8	2.00	1.217
6	125.7 (3)	54.1	2.32	0.903

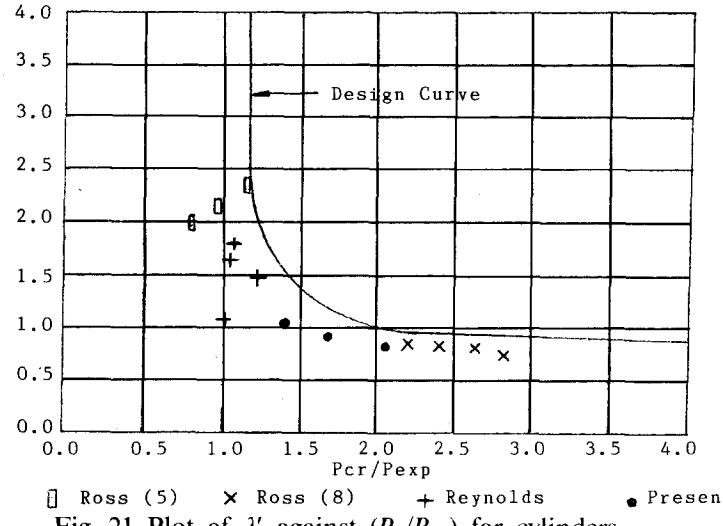

Fig. 21 Plot of λ' against (P_{cr}/P_{exp}) for cylinders.

4. Conclusions

The design curves of Figs. 21 and 22 appear to be quite useful for design pruposes, although for practical cases, the curves would lie higher than those shown, because the initial out-of-circularity/equivalent thickness ratios for welded full scale vessels is likely to be relatively larger than those of the machined models. The effects of initial out-of-circularity should proves less detrimental to vessels whose λ' is larger than 1.8.

It is considered that for the present series of models, where the initial out-of-circularity is very small and of a random shape, the vessels initially suffered plastic axisymmetric deformation in the circumferential direction, causing the tangent modulus to be considerably less than the elastic modulus. The result of this reduced the modulus in the circumferential direction and caused the vessels to fail through plastic general instability at a pressure considerably less than the theoretical predictions based on elastic theory.

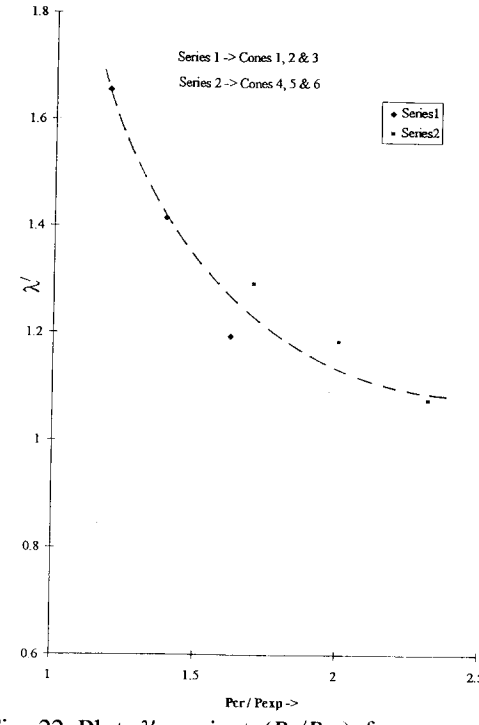

Fig. 22 Plot λ' against (P_{cr}/P_{exp}) for cones.

Acknowledgements

The author would like to thank Paul Haynes, Hugh Hamer and Terry Johns for their assistance. His thanks are extended to Dr Monty Bedford for his encouragement.

Lastly, but not leastly, the author would like to thank Miss Sharon Snook for the care and devotion she showed in typing this manuscript.

References

Bosman, T.N., Pegg, N.G., Kenning, P.J. (1993), "Experimental and numerical determination of non-linear overall collapse of imperfect pressure hull compartments", *RINA*, London.

Galletly, G.D., Slankard, R.C. and Wenk, E. (1958), "General instability of ring-stiffened cylindrical shells subject to external hydrostatic pressure-a comparison of theory and experiment", *J Appl Mechs, ASME*, 259-266, June.

Kendrick, S. (1953), "The buckling under external pressure of circular cylindrical shells with evenly spaced equal strength circular ring frames-Part I", *NCRE Report* No R211.

Nash, W.A. (1954), "General instability of ring-reinforced shells subject to hydrostatic pressure", *Proc 2nd US National congress on Applied Mechanics*, 359-368, June.

Reynolds, T.E. and Blumenberg, W.F. (1959), "General instability of ring-stiffened cylindrical shells subject to external hydrostatic pressure", DTMB, Structural Mechanics Lab, Research and Development Report, Report 1324.

Ross, C.T.F., "The collapse of ring-stiffened cylinders under uniform external pressure", *RINA* 1965.

Ross, C.T.F. (1976), "Vibration and instability of ring-stiffened circular cylinders and conical shells". *J Ship Res*, **20**, 22-31 March.

Ross, C.T.F. (1990), *Pressure Vessel under External Pressure*, Chapman & Hall.
Ross, C.T.F. and Johns, T. (1988), "Buckling and vibration of ring-stiffened cones under uniform external pressure", *Thin-Walled Structures*, **6**, 321-342.
Ross, C.T.F., Aylward, W.R. and Boltwood, D.T. (1971), "General instability of ring-reinforced circular cylinders under external pressure", *Trans RINA*, **113**, 73-82.
Windenburg, D.F. and Trilling, C. (1934), "Collapse by instability of thin cylindrical shells under external pressure", *Trans ASME*, 819-825.